

Rapid communication

## Interfacial polymerization of thin film nanocomposites: A new concept for reverse osmosis membranes

Byeong-Heon Jeong<sup>a</sup>, Eric M.V. Hoek<sup>a,\*</sup>, Yushan Yan<sup>b</sup>, Arun Subramani<sup>b</sup>,  
Xiaofei Huang<sup>a</sup>, Gil Hurwitz<sup>a</sup>, Asim K. Ghosh<sup>a</sup>, Anna Jawor<sup>a</sup>

<sup>a</sup> Civil & Environmental Engineering Department and Water Technology Research Center,  
University of California, Los Angeles, CA 90095, USA

<sup>b</sup> Chemical and Environmental Engineering Department, University of California,  
Riverside, CA 92521, USA

Received 4 January 2007; received in revised form 4 February 2007; accepted 14 February 2007  
Available online 21 February 2007

### Abstract

Here, we report on a new concept for formation of mixed matrix reverse osmosis membranes by interfacial polymerization of nanocomposite thin films *in situ* on porous polysulfone supports. Nanocomposite films created for this study comprise NaA zeolite nanoparticles dispersed within 50–200 nm thick polyamide films. Hand-cast pure polyamide membranes exhibit surface morphologies characteristic of commercial polyamide RO membranes, whereas nanocomposite membranes have measurably smoother and more hydrophilic, negatively charged surfaces. At the highest nanoparticle loadings tested, hand-cast nanocomposite film morphology is visibly different and pure water permeability is nearly double that of hand-cast polyamide membranes with equivalent solute rejections. Comparison of membranes formed using pore-filled and pore-opened zeolites suggest nanoparticle pores play an active role in water permeation and solute rejection. The best performing nanocomposite membranes exhibit permeability and rejection characteristics comparable to commercial RO membranes. As a concept, thin film nanocomposite membrane technology may offer new degrees of freedom in tailoring RO membrane separation performance and material properties.

© 2007 Elsevier B.V. All rights reserved.

**Keywords:** Reverse osmosis; Interfacial polymerization; Zeolite; Polyamide; Mixed matrix; Nanocomposite

### 1. Introduction

Water is the backbone of the global economy—quality, reliable, and sustainable supplies are vital for agriculture, industry, recreation, energy production, and domestic consumption [1]. Improving the effectiveness and efficiency of water purification technology, to produce clean water and protect the environment in a sustainable manner, is considered by many *the* challenge of this century [2]. In recent years, reverse osmosis (RO) has become a critical water technology, which promises to greatly increase the supply of clean water through purification of non-traditional water sources. However, despite their elegant design, conventional RO membranes are largely based on polymer chemistry that is now more than 30 years old.

In the 1970s, composite membranes comprising ultra-thin polyamide films—formed via *in situ* polycondensation on porous polysulfone supports—were developed to replace integrally skinned, asymmetric RO membranes—formed by phase inversion of cellulose acetate [3,4]. A great advantage of thin film composite technology is that it allows development and successful handling of extremely thin layers of barrier materials formed from almost any conceivable chemical combination [5]. In addition, the ultra-thin barrier layer and the porous support can be independently optimized with respect to structure, stability, and performance.

Over the last 30 years, water flux and solute rejection by polyamide thin film composite (TFC) membranes have continually improved, but reverse osmosis processes remain relatively energy-intensive, non-selective, and fouling-prone. A lack of significant innovations in RO membrane materials persists despite the pressing needs for desalination membranes with (1) increased water permeability for energy savings, (2) improved

\* Corresponding author. Tel.: +1 310 206 3735; fax: +1 310 206 2222.  
E-mail address: [hoek@seas.ucla.edu](mailto:hoek@seas.ucla.edu) (E.M.V. Hoek).

control of selectivity in membrane design, and (3) more fouling resistant surfaces [6,7]. These constraints remain in the face of rising worldwide demand for clean water and the sustainability imperatives to control energy consumption.

Nanotechnology has produced entirely new classes of functional materials whose application to desalination and water purification need exploration. For example, recent reports on filtration and desalination membranes fabricated from carbon nanotubes [8–10] and zeolite films [11–13] offer exciting new possibilities. Mixed matrix or nanocomposite membranes may exhibit improved mechanical, chemical, and thermal stability as well as improved separation, reaction, and sorption capacity [14]. Mixed matrix membranes developed for gas separation, pervaporation, ion-exchange, and fuel cell applications employ zeolite or carbon molecular sieve particles disperse within relatively thick membrane films [15–19].

Here we report on a new concept, that is, interfacial polymerization of thin film nanocomposite (TFN) reverse osmosis membranes [20]. The goal, as depicted in Fig. 1, is to embed molecular sieve nanoparticles throughout the polyamide thin film layer of an interfacial composite RO membrane. Synthesized NaA zeolite nanoparticles, characterized by a super-hydrophilic and negatively charged three-dimensional molecular sieve pore network, are used as the dispersed nanophase. It is hypothesized that super-hydrophilic, negatively charged, molecular sieve zeolite nanoparticles will provide preferential flow paths for water permeation while maintaining high solute rejection through combination of steric and Donnan exclusion.

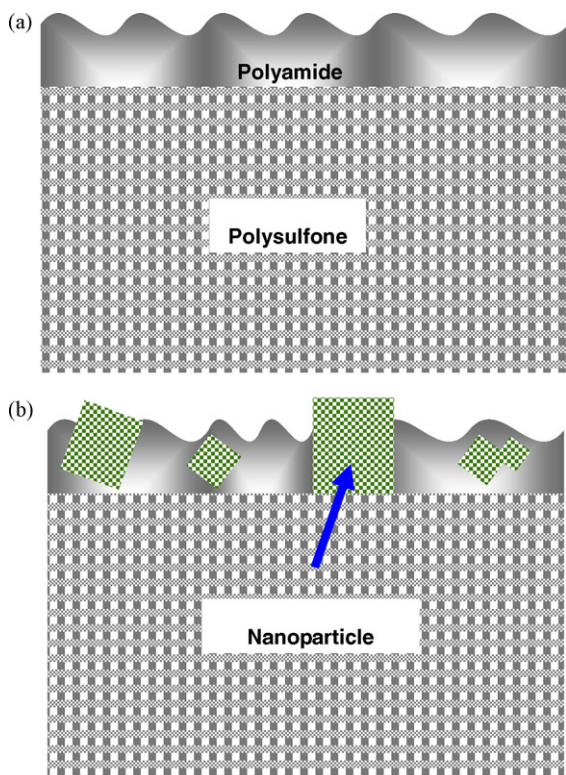


Fig. 1. Conceptual illustration of (a) TFC and (b) TFN membrane structures.

## 2. Experimental

### 2.1. Nanoparticle synthesis

Zeolite nanoparticles (NaA-type) were synthesized from the  $\text{Na}_2\text{O}-\text{SiO}_2-\text{Al}_2\text{O}_3-\text{H}_2\text{O}$  system with the use of an organic template (tetramethylammonium hydroxide) by a hydrothermal reaction according to previously published procedures [19,21]. The as-synthesized zeolite A nanoparticles are pore-filled because the presence of the template inside the zeolite pore structures. Pore-opened zeolite nanoparticles were obtained from the pore-filled particles by removing the template by calcinations, assisted by a polymer network as designed as a temporary barrier to prevent nanoparticle aggregation during the calcination process [22].

### 2.2. Nanoparticle characterization

The crystalline structure and the mean hydrodynamic diameter of synthesized zeolite A nanoparticles were evaluated by powder X-ray diffraction, XRD (Bruker AXS D8 diffractometer using  $\text{Cu K}\alpha$  radiation) and dynamic light scattering (BI-90 Plus, Brookhaven Instruments Corp.), respectively. Zeolite nanoparticles were dispersed in deionized laboratory water for light scattering measurements. Zeta potentials of synthesized zeolite nanoparticles were calculated from electrophoretic mobility measurements (ZetaPALS, Brookhaven Instruments Corp.) in 10 mM NaCl solution at unadjusted pH ( $\sim 5.8$ ). Morphological characterization of zeolite nanoparticles was carried out using scanning electron microscopy, SEM (Hitachi S-4700). Samples were sputter-coated with a mixture of gold and palladium. Energy dispersive X-ray (EDX) spectroscopy (equipped with the SEM) was used to determine the Si/Al ratio and elemental compositions of nanoparticles.

### 2.3. Membrane formation

Both TFC and TFN membranes were hand-cast on preformed polysulfone ultrafiltration (UF) membranes (provided by KRICT, Korea) through interfacial polymerization. A UF membrane taped to a glass plate was placed in an aqueous solution of 2% (w/v) *m*-phenylenediamine (MPD, >99%, Sigma–Aldrich) for approximately 2 min, and MPD soaked support membranes were then placed on a rubber sheet and rolled with a rubber roller to remove excess solution. The MPD saturated UF membrane was then immersed in a solution of 0.1% (w/v) trimesoyl chloride (TMC, 98%, Sigma–Aldrich) in hexane [23]. After 1 min of reaction, the TMC solution was poured off and the resulting membranes were rinsed with an aqueous solution of 0.2% (w/v) sodium carbonate ( $\text{Na}_2\text{CO}_3$ , HPLC grade, Fisher Scientific). Nanocomposite membranes were made by dispersing 0.004–0.4% (w/v) of synthesized zeolite A nanoparticles in the hexane–TMC solution. Nanoparticle dispersion was obtained by ultrasonication for 1 h at room temperature immediately prior to interfacial polymerization.

## 2.4. Membrane characterization

Images of thin film surface and cross-section were obtained using SEM (as described above) and transmission electron microscopy, TEM (JEOL 100CX), respectively. Membrane samples were prepared for TEM imaging by peeling away the polyester backing fabric, gently to ensure polysulfone and polyamide layers remained together. Small pieces of the fabric free membrane samples were embedded in Epon resin (Eponate 12, Ted Pella, Inc.). Approximately 60–80 nm thick sections were cut on a Reichert-Jung Ultracut E ultramicrotome and placed on Formvar-coated copper grids. The sections were examined at an accelerating voltage of 80 kV.

The surface (zeta) potential of hand-cast membranes was determined by measuring the streaming potential (BI-EKA, Brookhaven Instrument Corp.) with 10 mM NaCl solution at unadjusted pH ( $\sim 5.8$ ). Sessile drop contact angles of deionized water were measured on air dried samples of synthesized membranes in an environmental chamber mounted to the contact angle goniometer (DSA10, KRÜSS). The equilibrium value was the steady-state average of left and right angles. Surface roughness of the synthesized membranes was measured by AFM (Nanoscope IIIa, Digital Instruments). A silicon nitride cantilever tip (NSC 14, MikroMasch) was used at a fixed scanning rate of 1 Hz. The tip radius was less than 10 nm, and the cantilever length was 125  $\mu\text{m}$  with a spring constant of 5 N/m. In the operation of AFM, membrane surfaces were scanned in tapping mode, which is appropriate for soft polymers [24].

Twelve measurements were made on three samples of each membrane synthesized on three separate occasions. Average values for each membrane were computed after dropping the highest and lowest measured values.

Separation performance of the membranes was evaluated in terms of pure water flux and solute rejection in a high-pressure chemical resistant stirred cell (HP4750 Stirred Cell, Sterlitech Corp.). The effective membrane area was 13.85  $\text{cm}^2$ . The pure water flux was measured at room temperature ( $\sim 20^\circ\text{C}$ ) after the membranes were compressed for 3 h at 1.24 MPa. The solute rejection test was then carried out with 2000 ppm aqueous solutions of polyethylene glycol with average molecular weight of 200 g/mol (PEG 200), as well as 2000 ppm aqueous solutions of NaCl and  $\text{MgSO}_4$  at the same pressure. Solute rejection was obtained from the average of initial and final feed concentrations and the average permeate concentration at a permeate recovery of 50%. Four coupons from each membrane were evaluated to determine average water permeability and solute rejections. Three commercial RO membranes (SWHR, XLE, and NF90; FilmTec Corp. Edina, MN) were also characterized following identical procedures.

## 3. Results and discussion

The morphology of synthesized nanoparticles is illustrated in Fig. 2(a). The crystal structure of the same nanoparticles is confirmed to be pure zeolite A according to the X-ray diffraction (XRD) pattern in Fig. 2(b) when compared to standards developed by the Joint Committee on Powder Diffraction Standards

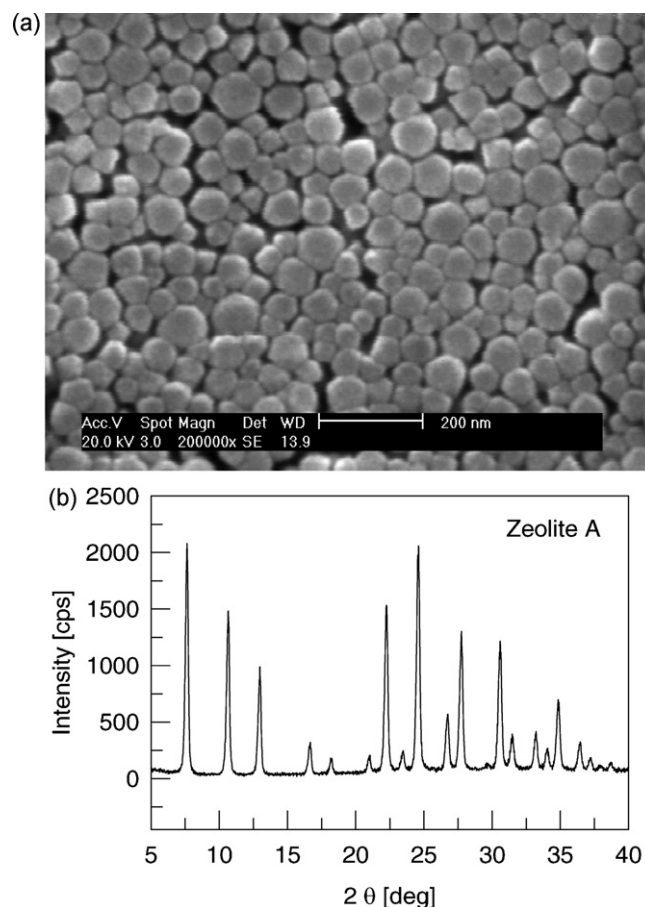


Fig. 2. Properties of synthesized zeolite nanoparticles by (a) SEM and (b) XRD.

(<http://www.icdd.com>) [19]. Synthesized zeolite A nanoparticles exhibit particle sizes range from  $\sim 50$  to  $\sim 150$  nm with mean hydrodynamic diameter of 100 nm confirmed by dynamic light scattering.

In general, zeolites with lower Si/Al ratios are more hydrophilic and have higher (negative) charge densities. The negative charge is compensated by cations located in the intracrystalline channels and cavities, but not necessarily on their surfaces when dispersed in aqueous electrolytes. The Si/Al ratio of synthesized zeolite nanoparticles was found to be 1.5 by energy dispersive X-ray (EDX) spectroscopy. Pore-opened zeolite nanoparticles exhibit a zeta potential of  $-72 \pm 4$  mV when immersed in an aqueous 10 mM NaCl solution at pH  $\sim 6$ . Grown films of zeolite A are super-hydrophilic with sessile drop water contact angles less than  $5^\circ$  [25]. Synthesized zeolites are NaA-type, and thus, have entrance pores of approximately 4 Å [26]. Hence, these small, super-hydrophilic, negatively charged pores are highly attractive to water, but highly repulsive to anions due to Coulombic repulsion [27].

Transmission electron microscope images and EDX spectra are presented for pure polyamide TFC membranes in Fig. 3(a) and (b) and for zeolite-polyamide TFN membranes in Fig. 3(c) and (d). Both TFC and TFN membranes exhibit nano-scale surface roughness, which is a well-known characteristic of interfacially polymerized polyamide RO membranes [24,28]. The irregular morphology precludes quantification of a single film

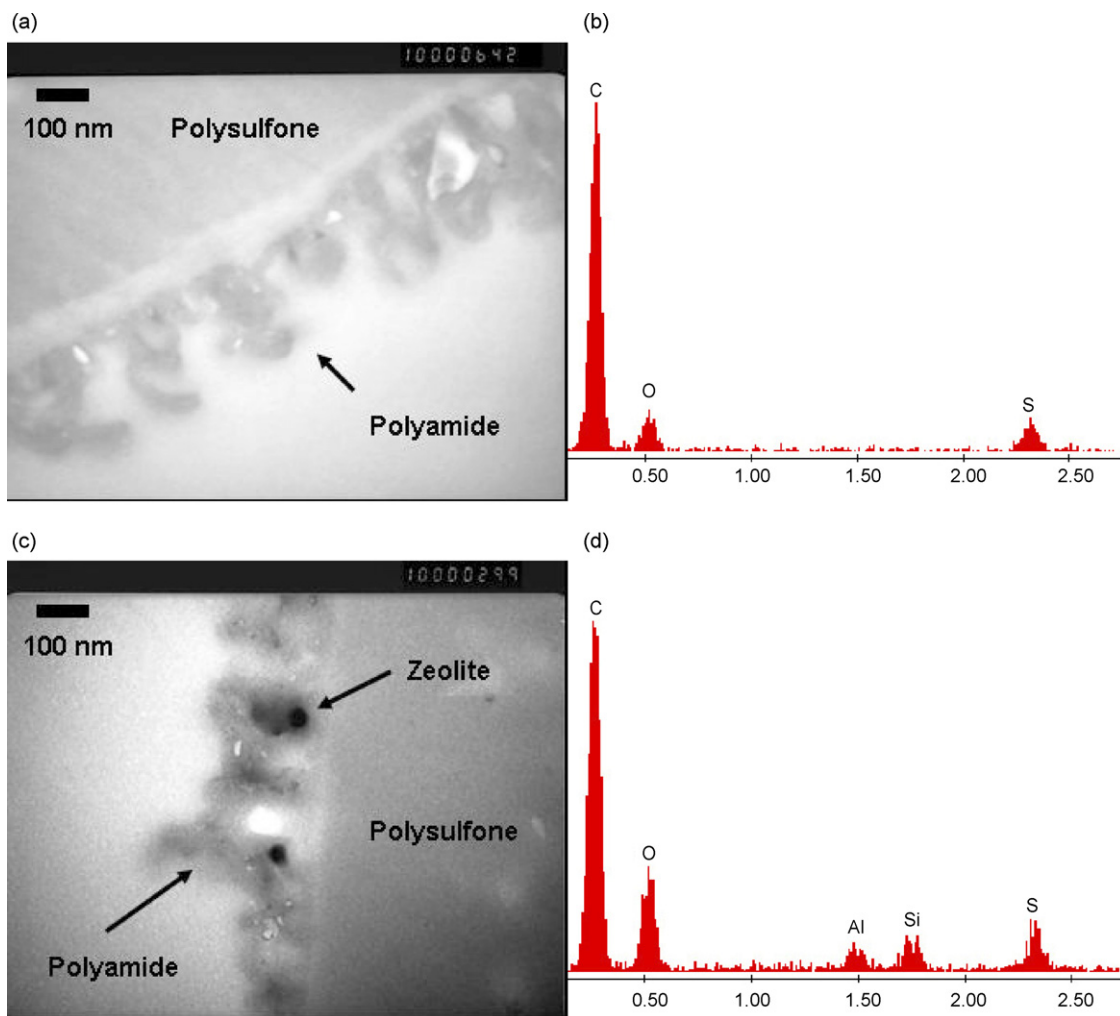


Fig. 3. Characterization of hand-cast thin film properties by TEM and EDX for (a–b) pure polyamide membrane and (c–d) nanocomposite membrane. Magnification is 100,000 $\times$  in TEM images.

layer thickness, but both thin films are about 50–200 nm. In Fig. 3(c), zeolite nanoparticles appear considerably darker than the polymer and are clearly located within the cross-section of the thin film, but also at the interface. The EDX spectrum in Fig. 3(d) indicates the Al peak at  $\sim 1.49$  keV and Si peak at  $\sim 1.74$  keV, confirming the presence of the zeolite nanoparticles, which are absent from the pure TFC film in Fig. 3(a) and the corresponding EDX spectrum in Fig. 3(b). Furthermore, the O peak at  $\sim 0.53$  keV is greater in the TFN membrane than in the TFC membrane due to oxygen atoms contained in the zeolite framework. The sulfur peak is from the polysulfone support on which both films were cast.

Fig. 4(a)–(f) are SEM images of synthesized TFC and TFN membrane surfaces. The five TFN membranes depicted in Fig. 4(b)–(f) were synthesized with increasing nanoparticle loadings. At zero and low nanoparticle loadings, depicted in Fig. 4(a) and (b), surfaces of both TFC and TFN membranes exhibit the familiar “hill and valley” structure of polyamide RO membranes [28]. At higher zeolite loadings, Fig. 4(c)–(f), but particularly Fig. 4(f), zeolite nanoparticles are visible on the membrane surface. Three white circles in Fig. 4(f) are drawn

around features believed to be zeolite nanoparticles because of their more “cubic” shape, which is consistent with the morphology of zeolite A nanoparticles. Also, EDX analysis confirms nanoparticle presence at discrete locations within the film layer and at the interface.

Measured values of TFC and TFN membrane surface roughness, water contact angle, and surface (zeta) potential are plotted in Fig. 5(a). In general, as nanoparticle loading increases, TFN membranes become smoother, more hydrophilic, and more negatively charged. Most significant is the reduction in contact angle, which is normally interpreted as an increase in hydrophilicity, from about  $70^\circ$  for the pure polyamide to about  $40^\circ$  for the nanocomposite with the highest nanoparticle loading. The combination of relatively smooth, hydrophilic, and negatively charged film layer typically produces better water permeability, salt rejection, and fouling resistance in water purification applications [24].

In Fig. 5(b), pure water permeability of TFN membranes increases from  $2.1 \pm 0.1 \times 10^{-12} \text{ m Pa}^{-1} \text{ s}^{-1}$  (same as the TFC membrane) at the lowest zeolite loading, up to  $3.8 \pm 0.3 \times 10^{-12} \text{ m Pa}^{-1} \text{ s}^{-1}$  at the highest zeolite loading.

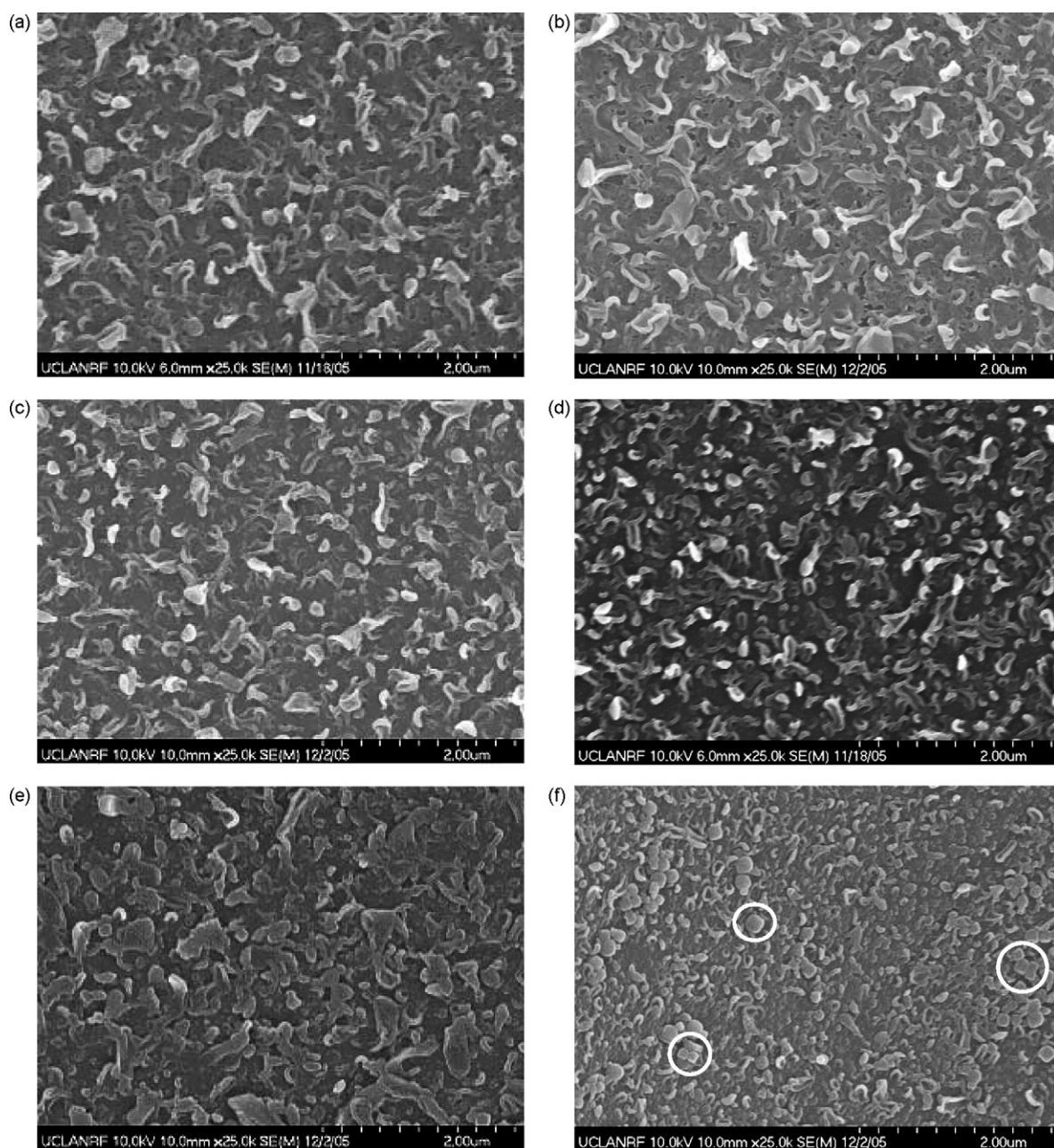


Fig. 4. SEM images of (a) TFC and (b–f) TFN membrane surfaces. Nanoparticle loadings are (a) 0.0%, (b) 0.004%, (c) 0.01%, (d) 0.04%, (e) 0.1%, and (f) 0.4% (w/v).

Observed solute rejections of hand-cast membranes are all in excess of 90% at 50% recovery. The expected permeability-rejection tradeoff is not observed for TFN membranes. It is possible that solute rejection by more permeable TFN membranes would be slightly lower if rejection tests are conducted at constant flux instead of constant pressure in the dead end filtration cell. However, all rejections should be higher if evaluated in a spiral wound element operating at low recovery with a reasonable rate of crossflow over the membrane.

An additional set of TFN membranes were prepared with identical membrane formation conditions using pore-filled zeolite nanoparticles (i.e., the template was not removed before nanocomposite thin film formation). Pure water permeability

of pore-filled TFN membranes ( $2.5 \pm 0.1 \times 10^{-12} \text{ m Pa}^{-1} \text{ s}^{-1}$ ) is lower than the corresponding pore-opened TFN membranes ( $2.8 \pm 0.2 \times 10^{-12} \text{ m Pa}^{-1} \text{ s}^{-1}$ ). The lower water permeability suggests zeolite nanoparticle pores play an active role in water permeation through TFN membranes. However, the water permeability of pore-filled zeolite nanoparticles was also higher than pure polyamide TFC membranes ( $2.1 \pm 0.1 \times 10^{-12} \text{ m Pa}^{-1} \text{ s}^{-1}$ ).

We cannot rule out the presence and potential contribution to water permeation of molecular-scale voids between nanoparticles and the polymer; however, there are no significant differences in NaCl rejections of pore-filled and pore-opened TFN membranes. Zeta potentials of pore-filled and pore-opened

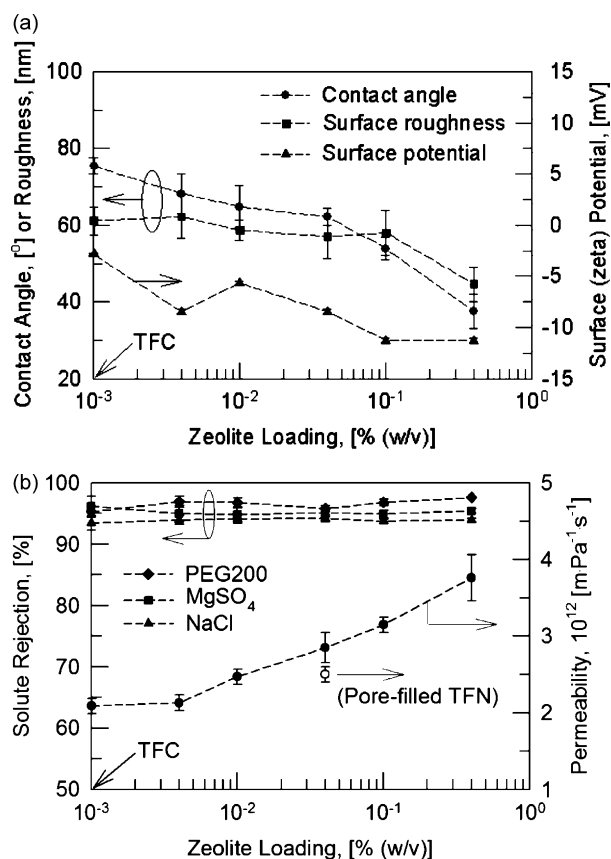


Fig. 5. Effect of zeolite loading on (a) surface properties and (b) separation performance of synthesized TFC and TFN membranes. Note: TFC data are plotted at 10<sup>-3</sup> for convenience.

zeolite nanoparticles are also statistically insignificant (data not shown); hence, we suggest that Donnan exclusion is enhanced for nanocomposite membranes through their more negative zeta potentials. In addition, as illustrated in Fig. 3(a) and (c), nanocomposite thin films exhibit different cross-sectional morphology, which might indicate changes in the polyamide film structure. Changes in glassiness of polymers in nanocomposites have been reported elsewhere [29].

Finally, in Table 1, pure water permeability and NaCl rejection of hand-cast TFC and TFN membranes are compared to three commercial RO membranes. The hand-cast TFN membrane exhibits the highest rejection and an intermediate permeability. It is not clear how the properties of TFN membranes might change if formed via modern commercial manufacturing methods, which often employ specially designed support membranes as well as additives to monomer solu-

Table 1  
Hand-cast and commercial membrane separation performance

Membrane designation	NP loading (% w/v)	Permeability (10 <sup>12</sup> m/Pa s)	NaCl rejection (%)
TFC	n/a	2.1 ± 0.1	93.4 ± 1.1
SWHR	n/a	2.6 ± 0.3	92.0 ± 1.9
TFN-400	0.400	3.8 ± 0.3	93.9 ± 0.3
XLE	n/a	16.8 ± 0.8	93.0 ± 1.2
NF90	n/a	27.7 ± 1.7	75.2 ± 3.1

tions that influence monomer solubility or hydrolysis, scavenge polymerization byproducts, and alter organic-water miscibility and interfacial tension. Once formed, commercial membranes are subject to a series of proprietary physical and chemical treatments (chemical rinses, heat curing, chlorination, etc.). Hand-cast membranes evaluated herein have not been optimized for use in practical reverse osmosis applications, but nanocomposite membrane technology offers new degrees of freedom to design RO membranes with properties, potentially, not attainable from polymeric materials alone.

#### 4. Conclusions

We demonstrate formation of zeolite-polyamide nanocomposite thin films by interfacial polymerization, which resulted in reverse osmosis membranes with dramatically improved permeability and interfacial properties when compared to similarly formed pure polyamide thin films. This new concept combines important properties of conventional membrane polymers (flexibility, ease of manufacture, high packing-density modules) with the unique functionality of molecular sieves (tunable hydrophilicity, charge density, pore structure, and antimicrobial capability along with better chemical, thermal, and mechanical stability). Water molecules appear to flow preferentially through super-hydrophilic, molecular sieve nanoparticle pores, while solute rejection remains comparable to pure polyamide membranes. We believe thin film nanocomposite materials represent a breakthrough in the design of reverse osmosis membranes - introducing new degrees of freedom in membrane design, which could lead to the next generation of high performance reverse osmosis membranes.

#### Acknowledgements

Financial support for this research was provided by the University of California and the Henry Samueli Fund at UCLA. We thank Dr. In-Chul Kim of Korea Research Institute of Chemical Technology (KRICT) for providing the polysulfone support membranes and for many useful discussions regarding synthesis of polyamide films. We are also grateful to Mary Cilluffo of the UCLA Brain Research Institute's Electron Microscopy Core Facility for help in preparing membrane samples for TEM imaging. Finally, we thank Prof. Yoram Cohen in the Department of Chemical & Biomolecular Engineering at UCLA for use of his AFM.

#### References

- [1] V. Gewin, Industry lured by the gains of going green, *Nature* 436 (2005) 173.
- [2] M. Elimelech, The global challenge for adequate and safe water, *J. Water Supply Res. Technol.* -Aqua 55 (2006) 3.
- [3] J.E. Cadotte, Interfacially synthesized reverse osmosis membrane, US Patent 4,277,344 (1981).
- [4] S. Loeb, S. Sourirajan, High flow porous membranes for separating water from saline solutions, US Patent 3,133,132 (1964).
- [5] J.E. Cadotte, R.J. Petersen, R.E. Larson, E.E. Erickson, New thin-film composite seawater reverse-osmosis membrane, *Desalination* 32 (1980) 25.

- [6] M.M. Clark, S. Allgeier, G. Amy, S. Chellam, F. Digiano, M. Elimelech, S. Freeman, J. Jacangelo, K. Jones, J.M. Laine, J. Lozier, B. Marinas, R. Riley, J. Taylor, M. Thompson, J. Vickers, M. Wiesner, A. Zander, Committee report: membrane processes, *J. Am. Water Work Assoc.* 90 (1998) 91.
- [7] I.C. Escobar, E.M. Hoek, C.J. Gabelich, F.A. Digiano, Y.A. Le Gouellec, P. Berube, K.J. Howe, J. Allen, K.Z. Atasi, M.M. Benjamin, P.J. Brandhuber, J. Brant, Y.J. Chang, M. Chapman, A. Childress, W.J. Conlon, T.H. Cooke, I.A. Crossley, G.F. Crozes, P.M. Huck, S.N. Kommineni, J.G. Jacangelo, A.A. Karimi, J.H. Kim, D.F. Lawler, Q.L. Li, L.C. Schideman, S. Sethi, J.E. Tobiasson, T. Tseng, S. Veerapanemi, A.K. Zander, Committee Report: recent advances and research needs in membrane fouling, *J. Am. Water Work Assoc.* 97 (2005) 79.
- [8] D.S. Sholl, J.K. Johnson, Making high-flux membranes with carbon nanotubes, *Science* 312 (2006) 1003.
- [9] J.K. Holt, H.G. Park, Y.M. Wang, M. Stadermann, A.B. Artyukhin, C.P. Grigoropoulos, A. Noy, O. Bakajin, Fast mass transport through sub-2-nanometer carbon nanotubes, *Science* 312 (2006) 1034.
- [10] X.F. Wang, X.M. Chen, K. Yoon, D.F. Fang, B.S. Hsiao, B. Chu, High flux filtration medium based on nanofibrous substrate with hydrophilic nanocomposite coating, *Environ. Sci. Technol.* 39 (2005) 7684.
- [11] G. Li, E. Kikuchi, M. Matsukata, A study on the pervaporation of water-acetic acid mixtures through ZSM-5 zeolite membranes, *J. Membr. Sci.* 218 (2003) 185.
- [12] L.X. Li, J.H. Dong, T.M. Nenoff, R. Lee, Reverse osmosis of ionic aqueous solutions on a MFI zeolite membrane, *Desalination* 170 (2004) 309.
- [13] L.X. Li, J.H. Dong, T.M. Nenoff, R. Lee, Desalination by reverse osmosis using MFI zeolite membranes, *J. Membr. Sci.* 243 (2004) 401.
- [14] W.J. Koros, Evolving beyond the thermal age of separation processes: membranes can lead the way, *AIChE J.* 50 (2004) 2326.
- [15] T.M. Gur, Permselectivity of zeolite filled polysulfone gas separation membranes, *J. Membr. Sci.* 93 (1994) 283.
- [16] R. Kiyono, G.H. Koops, M. Wessling, H. Strathmann, Mixed matrix microporous hollow fibers with ion-exchange functionality, *J. Membr. Sci.* 231 (2004) 109.
- [17] E. Okumus, T. Gurkan, L. Yilmaz, Development of a mixed-matrix membrane for pervaporation, *Sep. Sci. Technol.* 29 (1994) 2451.
- [18] D.Q. Vu, W.J. Koros, S.J. Miller, Mixed matrix membranes using carbon molecular sieves. I. Preparation and experimental results, *J. Membr. Sci.* 211 (2003) 311.
- [19] H.T. Wang, B.A. Holmberg, Y.S. Yan, Homogeneous polymer-zeolite nanocomposite membranes by incorporating dispersible template-removed zeolite nanocrystals, *J. Mater. Chem.* 12 (2002) 3640.
- [20] E.M.V. Hoek, B.H. Jeong, Y. Yan, Nanocomposite membranes and methods of making and using same, U.S. Application 11/364,885, Priority: US 60/660,428, March 9, 2005.
- [21] S. Mintova, N.H. Olson, V. Valtchev, T. Bein, Mechanism of zeolite a nanocrystal growth from colloids at room temperature, *Science* 283 (1999) 958.
- [22] H.T. Wang, Z.B. Wang, Y.S. Yan, Colloidal suspensions of template-removed zeolite nanocrystals, *Chem. Commun.* 23 (2000) 2333.
- [23] A.P. Rao, S.V. Joshi, J.J. Trivedi, C.V. Devmurari, V.J. Shah, Structure-performance correlation of polyamide thin film composite membranes: effect of coating conditions on film formation, *J. Membr. Sci.* 211 (2003) 13.
- [24] E.M. Vrijenhoek, S. Hong, M. Elimelech, Influence of membrane surface properties on initial rate of colloidal fouling of reverse osmosis and nanofiltration membranes, *J. Membr. Sci.* 188 (2001) 115.
- [25] A.M.P. McDonnell, D. Beving, A.J. Wang, W. Chen, Y.S. Yan, Hydrophilic and antimicrobial zeolite coatings for gravity-independent water separation, *Adv. Funct. Mater.* 15 (2005) 336.
- [26] D.W. Breck, *Zeolite Molecular Sieves*, John Wiley and Sons, New York, 1974.
- [27] R.M. Barrer, S.D. James, Electrochemistry of crystal-polymer membranes. I. Resistance measurements, *J. Phys. Chem.* 64 (1960) 417.
- [28] E.M.V. Hoek, S. Bhattacharjee, M. Elimelech, Effect of membrane surface roughness on colloid-membrane DLVO interactions, *Langmuir* 19 (2003) 4836.
- [29] T.C. Merkel, B.D. Freeman, R.J. Spontak, Z. He, I. Pinnau, P. Meakin, A.J. Hill, Ultrapermeable, reverse-selective nanocomposite membranes, *Science* 296 (2002) 519.